Cross Resonant Optical Antenna

P. Biagioni,[1,*] J. S. Huang,[1] L. Duò,[2] M. Finazzi,[2] and B. Hecht[1,†]

[1]Nano-Optics and Biophotonics group, Department of Experimental Physics 5, Wilhelm-Conrad-Röntgen-Center for Complex Material Systems (RCCM), Physics Institute, University of Würzburg, Am Hubland, 97074 Würzburg, Germany

[2]LNESS—Dipartimento di Fisica, Politecnico di Milano, Piazza Leonardo da Vinci 32, 20133 Milano, Italy

(Received 19 December 2008; revised manuscript received 5 March 2009; published 22 June 2009)

We propose a novel cross resonant optical antenna consisting of two perpendicular nanosized gold dipole antennas with a common feed gap. We demonstrate that the cross antenna is able to convert propagating fields of any polarization state into correspondingly polarized, localized, and enhanced fields and vice versa. The cross antenna structure therefore opens the road towards the control of light-matter interactions based on polarized light as well as the analysis of polarized fields on the nanometer scale.

DOI: 10.1103/PhysRevLett.102.256801 PACS numbers: 73.20.Mf, 68.37.Uv, 78.67.−n, 84.40.Ba

Polarized photons represent a fundamental probe to study the behavior of electrons in matter at optical frequencies, since they induce transitions that can be analyzed in terms of selection rules based on parity and angular momentum conservation. Optical fields with a well-defined polarization state are therefore of primary importance in many spectroscopic and microscopy applications [1]. For example, optical techniques widely used in solid state physics, like ellipsometry [1] or magneto-optical Faraday and Kerr effects [2], require the use of polarized laser beams, and sources of polarized single photons represent one of the building blocks of many quantum information processing concepts [3]. Nonlinear optical effects, such as second-harmonic generation, are also strongly polarization dependent [4,5]. The envisaged scaling down of all such applications to subdiffraction interaction volumes, as required by the ever-growing interest in nanostructured materials, will rely upon the availability of efficient sources of localized and enhanced polarized fields.

In this context, subwavelength apertures at the apex of metal-coated tapered fibers so far have been among the most used probes in scanning near-field optical microscopy (SNOM). However, fiber-based aperture probes suffer from very low throughput and strain-induced birefringence effects which can be detrimental for polarization-contrast techniques. Despite such drawbacks, SNOM setups with polarization control and analysis have been successfully implemented, and their application has been demonstrated for, e.g., magneto-optical imaging of magnetic films [6–8], polarimetry [9], linear dichroism mapping [10,11], fluorescence circular dichroism for spintronic applications [12], or single-emitter polarization mapping and control [13]. The use of hollow-pyramid SNOM probes has also been proposed in this context [14,15].

Over the last decade, noble metal nanostructures have become key elements for the engineering of enhanced and confined fields, as they combine geometrical effects (e.g., lightning-rod effects) with localized plasmon resonances, giving rise to large local intensity enhancement factors. The nanometer-scale modal volumes of such fields are ideally suited to promote the coupling to nanometer-scale emitters, like single molecules or quantum dots, leading to enhanced fluorescence [16,17] and spectroscopy [18]. Of particular relevance in this context are resonant optical antennas [19–26], since they potentially exhibit very strong localized fields in their feed gap, with local intensities enhanced by factors up to several thousand with respect to the incoming field. So far, mainly linear antennas (C_{2v} symmetry) have been proposed, either in the form of dipole antennas [19,24,25], bow-tie antennas [20,21], or monopole antennas [23]. However, the C_{2v} symmetry of linear antennas allows only one field component along the antenna axis to be present in the feed gap. Coupling to nanomatter is therefore restricted to transitions with dipole moment projections oriented along the antenna axis. Indeed, it has been recently shown experimentally that, for a single-molecule interacting with a linear optical antenna, the emitted polarization coincides with the antenna main axis rather than with the direction of the emitter transition dipole [27].

Moreover, a C_{2v} symmetry rules out experiments involving circularly polarized excitation and emission, which are a requirement for many envisaged applications such as the study of the response of chiral molecules [28], the study of spin dynamics and circularly polarized luminescence in semiconductor materials and devices for spintronic applications [12], as well as the scaling down to subdiffraction resolution of recent breakthroughs in opto-magnetic bit encoding via the inverse Faraday effect [29], which would allow ultrafast all-optical writing of nanometer-sized magnetic information.

In this Letter we propose a novel optical antenna configuration with fourfold (C_{4v}) symmetry, a cross antenna structure, consisting of two perpendicular dipole antennas with a common feed gap. We show by simulations that a cross antenna is able to confine and resonantly enhance polarized optical fields with high fidelity. Moreover, we demonstrate that the same structure can efficiently radiate polarized waves generated by a single dipole emitter, increasing its emission rate without perturbing its polarization pattern. From an experimental point of view, a resonant cross antenna may be structured on top of a flattened atomic-force microscopy tip [30] in order to scan it over a sample of interest. It should be pointed out that, in view of such applications, intensity distributions right outside the feed gap are a realistic description of the actual average intensity experienced by the sample.

The proposed concept rests upon the very basic knowledge that any arbitrary polarization state carried by a transverse propagating electromagnetic wave can be decomposed into two linear components, each one with the appropriate amplitude and phase. In this frame, two perpendicular linear antennas, with a common feed gap, are in principle able to sustain two such linear components, which are coherently added in the small volume of the feed gap.

A sketch of the here proposed antenna structure is shown in Fig. 1. We choose gold as the antenna material and use finite-difference time-domain simulations [31] in order to calculate the response of the cross antenna under excitation with a Gaussian beam or with a dipole source. We consider a wavelength of 800 nm for both far-field illumination and dipole emission, and take the complex permittivity of gold to be $\varepsilon = -26.64 + i1.66$ at this wavelength [32]. It should be stressed that the choice of a particular wavelength is arbitrary, and that the antenna geometry can always be tuned to match the desired resonance frequency, albeit other metals may have more favorable properties at other wavelengths. The antenna is residing on a fused silica substrate ($\varepsilon = 2.11$), while the upper half-space is vacuum. The antenna arms have a cross section of $20 \times 20\ \mathrm{nm}^2$ and a tip-to-tip distance (feed gap size) of 10 nm. A three-dimensional mesh of $0.5 \times 0.5 \times 0.5\ \mathrm{nm}^3$ is used for the simulations.

Once the antenna geometry has been chosen, the first step is to find the correct arm length to make the structure resonant at the desired wavelength (800 nm). In order to determine this value, we perform a first set of simulations where the arm length is varied while all other parameters are fixed. The structure is illuminated with a circularly polarized wave, without loss of generality. From the results of each simulation for a particular length, we then extract the field intensity in the feed gap center and take this intensity enhancement factor as a figure of merit for the antenna. In this way, we obtain the graph shown in Fig. 2(a), from which the resonant length for the two crossed dipole antennas is found to be around 170 nm. All the following simulations are performed using this length value, and the corresponding structure will be referred to as a resonant antenna. The intensity distributions for such an antenna, calculated at midheight of the antenna structure ($z = 10$ nm) and 5 nm above the upper antenna surface ($z = 25$ nm), are shown in Figs. 2(b) and 2(c), respectively, providing evidence that for a resonant antenna the field is highly enhanced and almost fully confined to the feed gap area. Exactly the same resonance curve is obtained when the antenna is illuminated with linearly polarized light, and the results obtained here for circularly polarized illumination can be directly extended to any polarization state.

In order to analyze the polarization response of the resonant cross antenna, we explicitly study the relevant case of illumination with circularly polarized light. Figure 3(a) displays again the experimentally relevant total field intensity I after circularly polarized illumination, calculated 5 nm above the upper antenna surface ($z = 25$ nm). Here we concentrate on the feed gap area where the electromagnetic energy is effectively confined. The performance of a source of circularly polarized photons is usually charac-

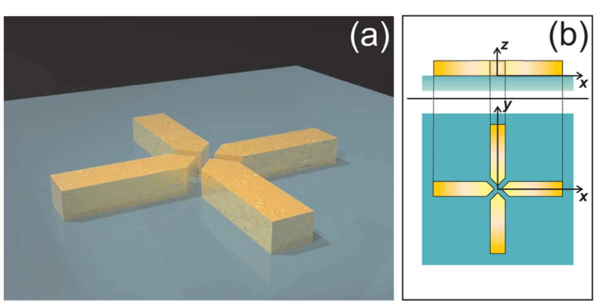

FIG. 1 (color online). Sketch of the proposed cross antenna structure (a) and of the reference frame used throughout the Letter (b).

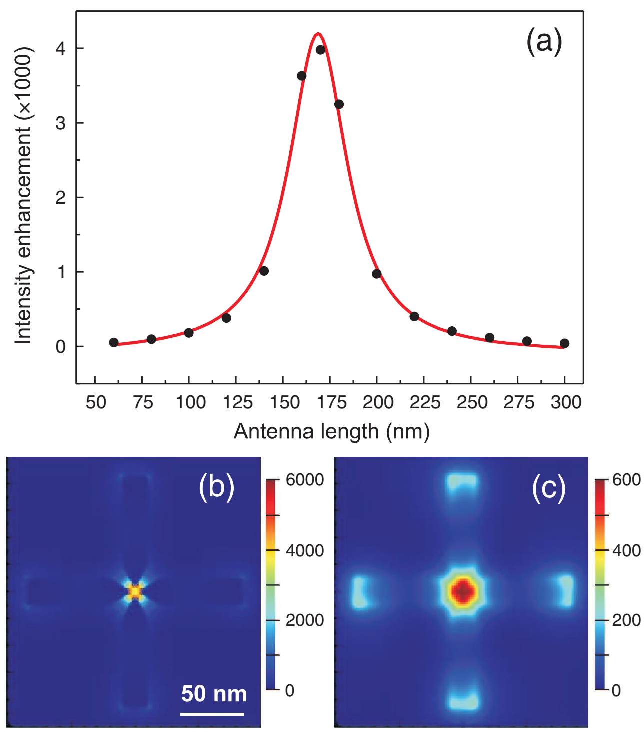

FIG. 2 (color online). (a) Resonant behavior of field intensity in the middle of the feed gap as a function of the antenna length after circularly polarized illumination (dots are results from simulations, and solid line is a guide for the eye); (b) intensity enhancement in a plane at midheight in the feed gap ($z = 10$ nm); (c) intensity enhancement 25 nm above the glass surface ($z = 25$ nm, i.e., 5 nm above the upper antenna surface). The scale bar in (b) also applies to (c).

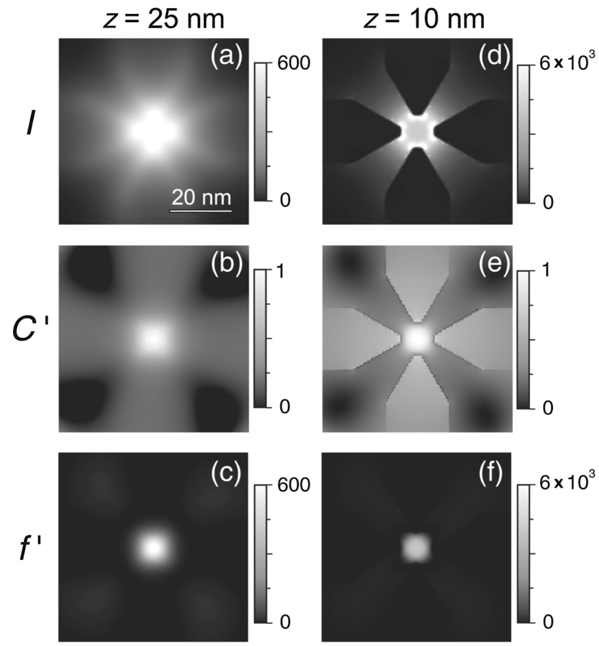

FIG. 3. Maps for the total intensity enhancement I (a, d), together with a map for the degree of circular polarization C' (b, e), and for the figure of merit f' (c, f), for far-field circularly polarized illumination with $C = +1$. The fields are monitored at $z = 25$ nm [i.e., 5 nm above the upper antenna surface, (a)–(c)] and at $z = 10$ nm [i.e., at midheight in the feed gap, (d)–(f)]. The scale bar in (a) also applies to all other panels.

terized by the figure of merit $f = I \times C^2$ [33], where C is the degree of circular polarization, defined for a quasimonochromatic plane wave propagating along the z direction as the ratio between the fourth and the first Stokes parameter [1], namely,

$$C = \frac{S_3}{S_0} = 2\frac{\langle E_x(t)E_y(t)\sin(\delta_x - \delta_y)\rangle}{\langle E_x^2(t)\rangle + \langle E_y^2(t)\rangle}, \tag{1}$$

where $\langle\cdot\rangle$ denotes time average, $E_x(t)$ and $E_y(t)$ are the electric field amplitudes, and $(\delta_x - \delta_y)$ their phase difference. When the antenna is illuminated by a wave propagating along the substrate normal, longitudinal field components will also be induced in its near field, and their presence must be taken into account as a possible source of background in the experiment. The concept of polarization degree for inhomogeneous waves characterized by a complex wave vector has been discussed previously, and it has been shown that generalized Stokes parameters should be introduced [34]. As we are interested in quantifying how much of the total near-field intensity is circularly polarized in the plane of the cross antenna, a very straightforward modification of C is suggested:

$$C' = 2\frac{\langle E_x(t)E_y(t)\sin(\delta_x - \delta_y)\rangle}{\langle E_x^2(t)\rangle + \langle E_y^2(t)\rangle + \langle E_z^2(t)\rangle}, \tag{2}$$

for which $|C'| < 1$ even for a perfect circular polarization in the xy plane, due to the presence of a spurious z component of the electric field. A spatial map for C' is calculated in Fig. 3(b), showing that a very uniform and nearly unitary degree of circular polarization is obtained throughout the whole feed gap area in a region roughly 10 nm in diameter (note that illumination with $C = +1$ is used in the simulations). We finally compute an accordingly modified figure of merit $f' = I \times (C')^2$, which is shown in Fig. 3(c), confirming that the cross antenna can be used as a local and enhanced source of circularly polarized photons. We would like to mention that numerical results for the same antenna structure show that for the experimentally less relevant midheight position inside the gap ($z = 10$ nm), part of the field intensity is located in four hot spots very close to the gold arms [see Fig. 3(d)], where boundary conditions force the fields to be mainly linearly polarized [see Figs. 3(e) and 3(f)]. Simulation results in the yz plane, showing the development of the field intensity and polarization at different heights in the feed gap, are presented in Ref. [35].

Finally, we study the emitting properties of the antenna by placing an emitter 5 nm above its upper surface, over the feed gap area. We show that, as opposed to linear antennas [27], our structure is able to preserve the far-field polarization pattern of an in-plane dipole with high fidelity. In order to analyze the emission properties of the antenna-coupled emitter, we record field components in a plane located 5 nm above the dipole, from which far-field patterns are calculated using the asymptotic form of the

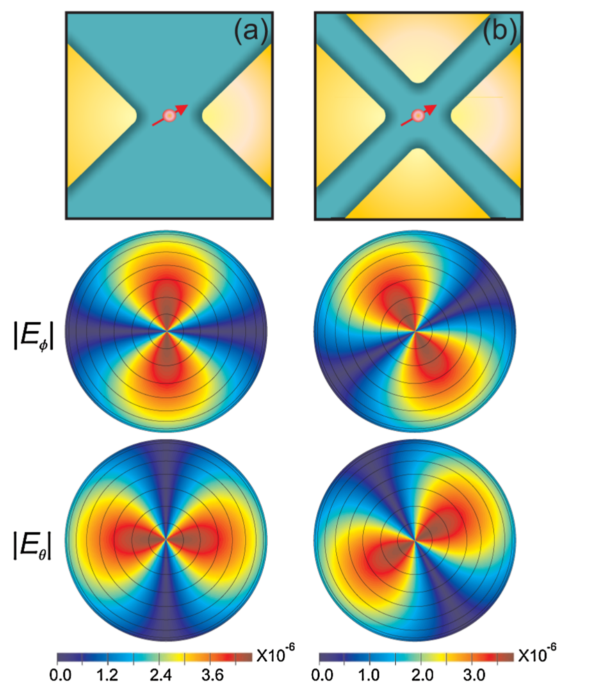

FIG. 4 (color online). Simulation results for an emitting dipole 5 nm above the upper antenna surface ($z = 25$ nm). Column (a): 30°-oriented dipole coupled to a resonant linear antenna structure (the antenna is oriented horizontally in the picture). Column (b): same as column (a), with the dipole coupled to a resonant cross antenna structure. Concentric circles in the plots for field components represent polar angular spread with steps of 10°.

angular spectrum of plane waves [36], which we use to project the field onto a sphere of 1 m radius. In Fig. 4(a) we show a sketch of a 30°-oriented in-plane dipole coupled to a resonant *linear* dipole antenna, together with the two transverse far-field components in polar coordinates, E_ϕ and E_θ (the antenna is oriented horizontally in the sketch). Simulations confirm that the polarization state in the far field is dictated by the direction of the antenna, rather than by the orientation of the emitting dipole [27]. We now couple the same dipole to a resonant *cross* antenna. Simulations, reported in Fig. 4(b), clearly show that the presence of the cross antenna in the near field of the emitter does not perturb the far-field polarization state of emitted waves, in contrast to the situation depicted in Fig. 4(a). We verified that such results hold independently of the in-plane dipole orientation and of its position in an area roughly 15 nm in diameter. Indeed, when the dipole is displaced horizontally by 8 nm and emission consequently drops by a factor of 5 because of weaker coupling to the antenna, still no significant changes can be seen in the far-field polarization pattern [35].

The antenna also provides an increase in the dipole emission rate, thanks to its ability to effectively link the antenna near field with the free space. In order to quantify this effect, we calculate and integrate the Poynting vector over the boundaries of the simulation area, with and without the antenna structure. In this way, we estimate an enhancement of the total radiated power by a factor of about 500 thanks to the presence of the resonant cross antenna. An even larger enhancement (about 2500) is found when the dipole is placed at midheight in the gap ($z = 10$ nm), although at this position the far-field polarization pattern is more sensitive to lateral displacements of the dipole. These enhancement factors compare very well with those found in the literature for simulated optimized linear dipole antennas [37].

It should be mentioned that, in view of experimental realizations, low-roughness structures must be selected, since near fields associated with imperfections can be detrimental for polarization-contrast techniques and should not extend too far outside the gap.

In conclusion, we have shown that a cross antenna structure, constituted by two perpendicular dipole antennas with a common feed gap, represents an effective way to squeeze polarized optical fields into subwavelength volumes with very large local intensity enhancements. Moreover, the same structure can efficiently radiate polarized waves from a single emitter, strongly increasing the total radiated power without affecting its polarization pattern. We envisage the realization of cross antenna structures by electron-beam lithography or focused ion-beam milling on top of atomic-force microscopy tips, thus providing an efficient scanning probe suitable for applying optical techniques with polarization control and analysis at the nanometer scale.

The authors wish to acknowledge T. Feichtner, A. Kimel, and M. Savoini for insightful discussions. Support from the European Nano Sci-ERA consortium and the Alexander von Humboldt Stiftung (P. B.) is gratefully acknowledged.

*paolo.biagioni@polimi.it
†hecht@physik.uni-wuerzburg.de

[1] R. M. Azzam and N. M. Bashara, *Ellipsometry and Polarized Light* (Elsevier Science B. V., Amsterdam, 1999).
[2] Z. Q. Qiu and S. D. Bader, J. Magn. Magn. Mater. **200**, 664 (1999).
[3] B. Lounis and M. Orrit, Rep. Prog. Phys. **68**, 1129 (2005).
[4] Y. R. Shen, *The Principles of Nonlinear Optics* (John Wiley and Sons, Hoboken, New Jersey, 2003).
[5] M. Finazzi, P. Biagioni, M. Celebrano, and L. Duò, Phys. Rev. B **76**, 125414 (2007).
[6] E. Betzig *et al.*, Appl. Phys. Lett. **61**, 142 (1992).
[7] P. Fumagalli *et al.*, Appl. Phys. Lett. **72**, 2803 (1998).
[8] W. Dickson *et al.*, Opt. Commun. **250**, 126 (2005).
[9] E. B. McDaniel, S. C. McClain, and J. W. P. Hsu, Appl. Opt. **37**, 84 (1998).
[10] T. Lacoste *et al.*, Ultramicroscopy **71**, 333 (1998).
[11] L. Ramoino *et al.*, Rev. Sci. Instrum. **73**, 2051 (2002).
[12] J. Levy *et al.*, Phys. Rev. Lett. **76**, 1948 (1996).
[13] R. J. Moerland *et al.*, Nano Lett. **8**, 606 (2008).
[14] S. Werner *et al.*, Appl. Phys. A **66**, S367 (1998).
[15] P. Biagioni *et al.*, Appl. Phys. Lett. **87**, 223 112 (2005).
[16] S. Kühn *et al.*, Phys. Rev. Lett. **97**, 017402 (2006).
[17] P. Anger, P. Bharadwaj, and L. Novotny, Phys. Rev. Lett. **96**, 113002 (2006).
[18] P. Olk *et al.*, Nano Lett. **7**, 1736 (2007).
[19] P. Mühlschlegel *et al.*, Science **308**, 1607 (2005).
[20] J. N. Farahani *et al.*, Phys. Rev. Lett. **95**, 017402 (2005).
[21] P. J. Schuck *et al.*, Phys. Rev. Lett. **94**, 017402 (2005).
[22] J. Alda *et al.*, Nanotechnology **16**, S230 (2005).
[23] T. H. Taminiau *et al.*, Nano Lett. **7**, 28 (2007).
[24] O. L. Muskens *et al.*, Nano Lett. **7**, 2871 (2007).
[25] E. Cubukcu *et al.*, Appl. Phys. Lett. **89**, 093 120 (2006).
[26] E. Cubukcu *et al.*, IEEE J. Sel. Top. Quantum Electron. **14**, 1448 (2008).
[27] T. H. Taminiau *et al.*, Nat. Photon. **2**, 234 (2008).
[28] M. Quack, Angew. Chem., Int. Ed. Engl. **28**, 571 (1989).
[29] C. D. Stanciu *et al.*, Phys. Rev. Lett. **99**, 047601 (2007).
[30] P. Biagioni *et al.*, Rev. Sci. Instrum. **79**, 016 103 (2008).
[31] *FDTD Solutions* v. 6.0.5, Lumerical Solutions Inc., Vancouver, Canada.
[32] P. B. Johnson and R. W. Christy, Phys. Rev. B **6**, 4370 (1972).
[33] T. Funk *et al.*, Coord. Chem. Rev. **249**, 3 (2005).
[34] T. Setälä *et al.*, Phys. Rev. E **66**, 016615 (2002).
[35] See EPAPS Document No. E-PRLTAO-103-022928. Figure 1: simulation results in the yz plane after far-field circular illumination. Figure 2: simulation results for a dipole emitter with different displacements along the x axis. For more information on EPAPS, see http://www.aip.org/pubservs/epaps.html.
[36] L. Novotny and B. Hecht, *Principles of Nano-Optics* (Cambridge University Press, Cambridge, England, 2006).
[37] L. Rogobete *et al.*, Opt. Lett. **32**, 1623 (2007).